ADVANCES IN ATMOSPHERIC SCIENCES, VOL. 37, JULY 2020, 671–678

• **Original Paper** •

Estimation of $PM_{2.5}$ Mass Concentration from Visibility

Denghui JI[1,5], Zhaoze DENG[*1,4], Xiaoyu SUN[1,5], Liang RAN[1,4], Xiangao XIA[1,4,5], Disong FU[1,5], Zijue SONG[1], Pucai WANG[1,4,5], Yunfei WU[2], Ping TIAN[3], and Mengyu HUANG[3]

[1]*Key Laboratory of Middle Atmosphere and Global environment Observation (LAGEO), Institute of Atmospheric Physics, Chinese Academy of Sciences, Beijing* 100029, *China*

[2]*Key Laboratory of Regional Climate-Environment for Temperate East Asia (RCE-TEA), Institute of Atmospheric Physics, Chinese Academy of Sciences, Beijing* 100029, *China*

[3]*Beijing Weather Modification Office, Beijing* 100089, *China*

[4]*Xianghe Observatory of Whole Atmosphere, Institute of Atmospheric Physics, Chinese Academy of Sciences, Xianghe* 065400, *China*

[5]*University of Chinese Academy of Sciences, Beijing* 100049, *China*

(Received 14 January 2020; revised 3 April 2020; accepted 15 April 2020)

ABSTRACT

Aerosols in the atmosphere not only degrade visibility, but are also detrimental to human health and transportation. In order to develop a method to estimate $PM_{2.5}$ mass concentration from the widely measured visibility, a field campaign was conducted in Southwest China in January 2019. Visibility, ambient relative humidity (RH), $PM_{2.5}$ mass concentrations and scattering coefficients of dry particles were measured. During the campaign, two pollution episodes, i.e., from 4–9 January and from 10–16 January, were encountered. Each of the two episodes could be divided into two periods. High aerosol hygroscopicity was found during the first period, when RH was higher than 80% at most of the time, and sometimes even approached 100%. The second period experienced a relatively dry but more polluted condition and aerosol hygroscopicity was lower than that during the first period. An empirical relationship between $PM_{2.5}$ mass concentration and visibility (ambient aerosol extinction) under different RH conditions could thus be established. Based on the empirical relationship, $PM_{2.5}$ mass concentration could be well estimated from visibility and RH. This method will be useful for remote sensing of $PM_{2.5}$ mass concentration.

Key words: visibility, hygroscopic growth, $PM_{2.5}$ mass concentration

Citation: Ji, D. H., and Coauthors, 2020: Estimation of $PM_{2.5}$ mass concentration from visibility. *Adv. Atmos. Sci.*, **37**(7), 671–678, https://doi.org/10.1007/s00376-020-0009-7.

Article Highlights:

- Aerosol hygroscopicity was found to decline during pollution episodes.
- An improved method for estimating $PM_{2.5}$ mass concentration from visibility and RH was established.

1. Introduction

With rapid development in China, air quality has become more of a concern as a result of the increase in energy consumption (Pui et al., 2014; Chan and Yao, 2008). Due to the increase in emissions from coal consumption and automobiles, $PM_{2.5}$ (particulate matter with aerodynamic diameters of less than 2.5 μm) mass concentrations, sulfur dioxide (SO_2) and nitrogen oxides (NOx = NO + NO_2) have an important impact on air quality in most urban areas (Chan and Yao, 2008; Kan et al., 2012). $PM_{2.5}$ could pose harmful effects on public health and also degrade visibility (Zhang et al., 2014).

Visibility is a measure of the distance at which an object or light can be clearly discerned (Watson, 2002; Zhang et al., 2014). The damaged visibility is a reflection of the low transparency of the atmosphere. Visibility can reach 300 km when only taking into account Rayleigh scattering and gas absorption (Watson et al., 2002). However, visibility is reduced to a few kilometers in the presence of particles (Chan et al., 1999; Song et al., 2013; Liu et al., 2019). Several studies have shown the relationship between the aerosol loading and visibility, which is relevant to the

* Corresponding author: Zhaoze DENG
Email: dengzz@mail.iap.ac.cn

mass concentration, chemical composition and the size distribution of aerosols (Wang et al., 2015; Zhou et al., 2016; Liu et al., 2019). The distribution of $PM_{2.5}$ mass concentrations varies dramatically in spatiotemporal dimensions, and therefore estimation of $PM_{2.5}$ mass concentrations using satellite-based remote sensing data is a promising method (Sun et al., 2019). In many previous studies, the relationship between the satellite data of aerosol optical depth (AOD) and in-situ measured surface $PM_{2.5}$ mass concentrations was investigated (van Donkelaar et al., 2006; Chelani, 2019; Sun et al., 2019). Zheng et al. (2017) analyzed the influential factors including the aerosol type, relative humidity (RH), planetary boundary layer height, wind speed and direction, and the vertical structure of aerosol distribution.

According to those previous studies, aerosol water uptake has a significant impact on the relationship between AOD and $PM_{2.5}$ (Zhao et al., 2019). Aerosol hygroscopic growth enhances the scattering ability of particles, and accelerates the formation of haze pollution. However, some numerical models still lack sufficient input data for aerosol hygroscopicity (Zhao et al., 2019). The hygroscopic enhancement factor f(RH) was defined as the ratio of aerosol optical properties such as aerosol extinction, aerosol scattering and aerosol backscattering between wet and dry (reference) conditions (Kotchenruther and Hobbs, 1998). f(RH) can be obtained from nephelometer measurements with different methods. Malm and Day (2001) employed a single nephelometer with an RH range of 35%–85%. For other studies, two parallel nephelometers with one operated at lower RH and another at higher RH were used (Pandolfi et al., 2018). However, previous methods cannot precisely obtain the aerosol hygroscopicity when RH reaches above 90%. Zhao et al. (2019) reported f(RH) with a wider range of RH between 30% and 96% using an improved nephelometer system. With the development of methods and instruments in this field, there are many studies that have demonstrated the relationship between aerosol hygroscopicity and RH in different seasons and places (Li et al., 2013; Chen et al., 2019; Zhao et al., 2019).

Based on previous studies, the IMPROVE (Interagency Monitoring of Protected Visual Environments) project provides a method to calculate aerosol loading from visibility (Ryan et al., 2005). However, this method is relatively complicated, involving detailed measurements of mass concentrations of several components. In this study, an empirical method was developed to calculate $PM_{2.5}$ mass concentration from visibility and RH in a certain area where light extinction was mainly contributed by $PM_{2.5}$.

2. Measurements and methods

2.1. *Site and instruments*

The experiment was conducted from 4–19 January 2019 in Changshou, Chongqing, in Southwest China. The site (29°49'N, 107°00'E; 266 m above sea level) is located in Yanjia Industrial Park surrounded by busy highways. It is about 51 km away from the city center of Chongqing.

A dust monitor (EDM 180, Grimm Aerosol) and an ambient particulate monitor (FH62C14, Thermo Scientific) were used to jointly measure the aerosol mass concentration. The FH62C14 instrument provided $PM_{2.5}$ mass concentrations at 1-h intervals. The EDM 180 instrument measured aerosol number concentrations in 31 particle size channels, and mass concentrations including PM_{10}, $PM_{2.5}$ and $PM_{1.0}$, with a temporal resolution of 6 s. The isothermal inlet was integrated with a nafion dryer, which was turned on at ambient RH above 55%. Several studies have reported the errors in the measurements of GRIMM EDM 180 (Ding et al., 2014; Xu, 2017). Thus, the GRIMM EDM 180 measurements were validated using FH62C14 measurements at a 1-h temporal resolution. A good correlation between $PM_{2.5}$ mass concentrations from GRIMM EDM 180 and FH62C14 was found. Then, the GRIMM EDM 180 data were corrected using the regression fit function and reported at a temporal resolution of 10 min.

A polar nephelometer (Aurora-4000, Ecotech) was used to measure the aerosol scattering coefficients at seven angle ranges at the wavelengths of 635 nm, 525 nm, and 450 nm at relatively dry RH (~35%). Full scattering coefficients were corrected based on the measurements for the angle range 9°–170° using the method proposed by Müller et al. (2011). Black carbon (BC) mass concentration was measured by an aethalometer (model AE31, MAGEE) (Hansen et al., 1984; Collaud Coen et al., 2010) at seven wavelengths of 370, 470, 520, 590, 680, 880 and 950 nm. Loading effects were corrected and absorption coefficients were obtained following the method in Ran et al. (2016). However, data availability was only 35% due to instrument malfunction. Visibility was measured by a PWD20 instrument (Vaisala Co.) at an interval of 1 min. Ambient RH was observed by the sensor attached to the Grimm EDM 180 instrument.

The Grimm EDM 180 and FH62C14 instruments were calibrated before and after the campaign. The results showed that the instruments were stable throughout the campaign. Aurora-4000 was calibrated routinely and zero-checked every day for the correction of the zero point. All data were filtered according to measurement logs and data consistency between instruments. A flow chart of the steps involved in the method, which will be detailed in section 2.2, is presented in Fig. 1.

2.2. *Aerosol scattering hygroscopic growth algorithms*

Aerosol scattering coefficient and complex refractive index are related to ambient RH. Measurements of total scattering coefficient and the simultaneous RH are used to indicate aerosol hygroscopic growth. Several studies have defined the hygroscopic enhancement factor for aerosol total scattering, f(RH), and aerosol back scattering, f_b(RH), in different cases (Sun et al., 2016). The hygroscopic enhancement factor, which considers light extinction by scattering and absorption of both aerosol and gas, is defined as follows:

$$f_\lambda(\mathrm{RH}) = \frac{b_{\mathrm{sp},\lambda}(\mathrm{RH})}{b_{\mathrm{sp},\lambda}(\mathrm{dry})} = \frac{b_{\mathrm{ext},\lambda}(\mathrm{RH}) - b_{\mathrm{ap},\lambda} - b_{\mathrm{ag},\lambda} - b_{\mathrm{sg},\lambda}}{b_{\mathrm{sp},\lambda}(\mathrm{dry})}, \quad (1)$$

where $b_{sp,\lambda}$ (RH) and $b_{sp,\lambda}$ (dry) are the aerosol scattering coefficient at wavelength λ in the ambient environment and under dry conditions; $b_{ext,\lambda}$ (RH) is the ambient extinction coefficient; $b_{ap,\lambda}$ is the aerosol absorption coefficient; $b_{ag,\lambda}$ is the gas absorption coefficient; and $b_{sg,\lambda}$ is the gas scattering coefficient.

Since the gas extinction contribution to total light extinction is much less than that of particles in such polluted regions (Chan et al., 1999) and aerosol absorption is usually much smaller than aerosol scattering, Eq. (1) can be simplified to:

$$f_\lambda(\mathrm{RH}) = \frac{b_{ext,\lambda}(\mathrm{RH})}{b_{sp,\lambda}(\mathrm{dry})}. \quad (2)$$

It is calculated from the measurements of ambient extinction coefficient, $b_{ext,\lambda}$(RH), at a certain RH and aerosol scattering coefficient, $b_{sp,\lambda}$(dry), under dry conditions (RH < 40%). The $b_{ext,\lambda}$(RH) at a certain wavelength (λ) is calculated from visibility (V) by the following equation:

$$b_{ext,\lambda} = \frac{3.91}{V}\left(\frac{\lambda}{0.55}\right)^{-q}, \quad (3)$$

where the coefficient q is determined by experiments.

Two fit functions, the dual-parameter fit equation (Hänel, 1976, 1980; Carrico, 2003; Zieger et al., 2011; Liu et al., 2019) and single-parameter equation (Hänel, 1980; Kotchenruther and Hobbs, 1998; Gassó et al., 2000; Liu et al., 2019), were used to establish the relationship between f_λ(RH) and RH. Aerosols that are metastable or on the upper branch of the hygroscopic growth hysteresis curve typically follow the dual-parameter power lower fit equation described by Kasten (1969):

$$f(\mathrm{RH}) = \alpha\left(1 - \frac{\mathrm{RH}}{100}\right)^{-\gamma}, \quad (4)$$

where α is a scale factor that normalizes the hygroscopic growth and γ represents the magnitude of the hygroscopic growth.

During the observational period, RH was frequently above 60%, with few records at low RH. Curve fitting will be misleading under such a condition. Thus, f(RH) under dry conditions, which is the ratio of dry extinction and scattering from the aethalometer and nephelometer, was added for the curve fitting.

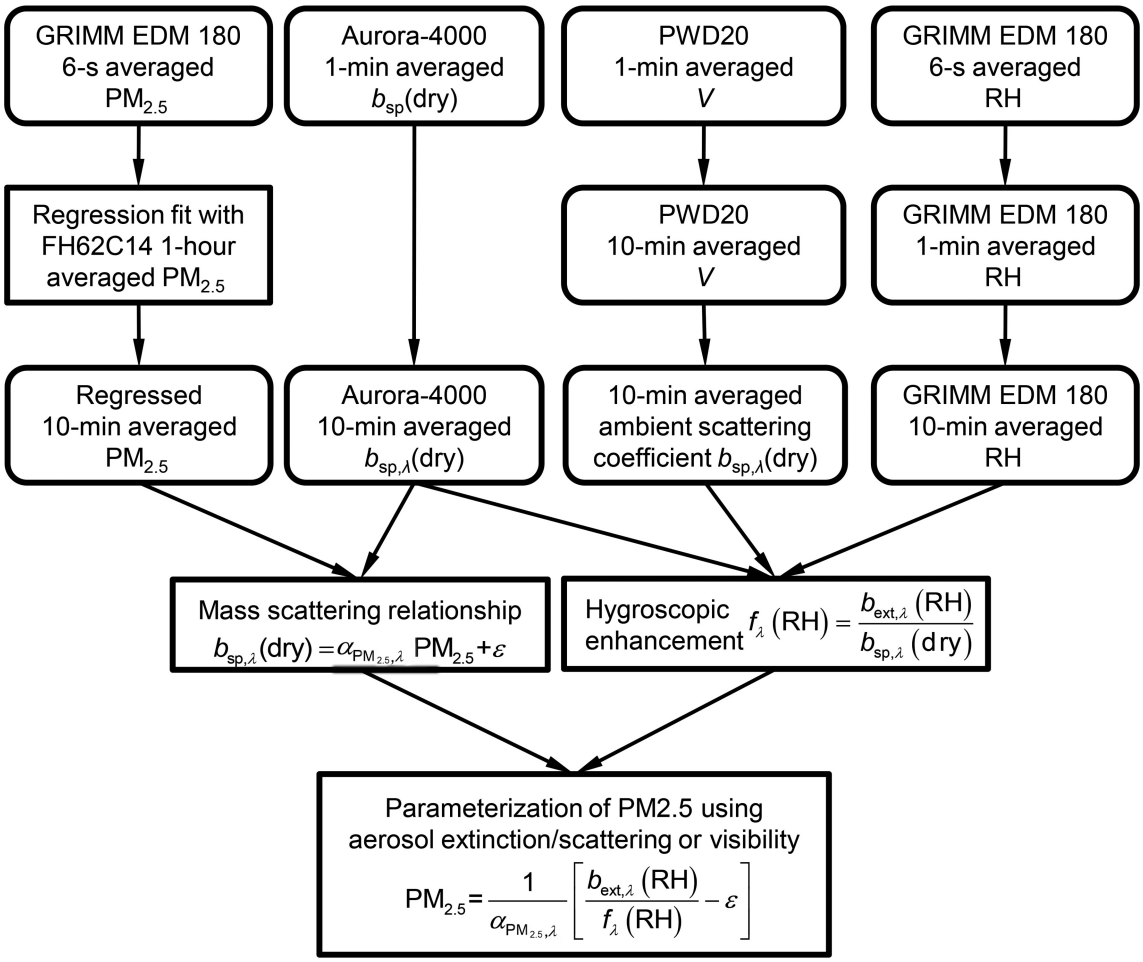

Fig. 1. Flow chart for data processing and parameterization.

3. Results and discussion

3.1. *Overview of the experiment*

Figure 2 shows the time series of $PM_{2.5}$ mass concentration, visibility, and RH during the experiment. It can be clearly seen that there were two episodes according to $PM_{2.5}$ mass concentrations, i.e., one from 4–9 January with a continuous increase from 75 μg m^{-3} to 200 μg m^{-3}, and the other from 10–16 January with an increase from 25 μg m^{-3} to 150 μg m^{-3}. A linear correlation between $PM_{2.5}$ mass concentration and dry aerosol scattering coefficient was found, with a correlation coefficient of about 0.98 (Fig. 3). However, there was no obvious decrease in visibility along with the increase in $PM_{2.5}$ mass concentration during either of the two episodes, as is often expected. No correlation between the mass concentration of $PM_{2.5}$ and visibility was found, with the correlation coefficient found to be 0.21. During the whole campaign, visibility ranged from 2 km to 15 km, with 86.4% lower than 10 km. It was notable that RH was higher than 70% at most of the time, and even up to 85%–100% during 53% of the whole time. Aerosol hygroscopic growth in such a highly humid environment may greatly influence the scattering properties of aerosol and thereby visibility.

3.2. *Aerosol hygroscopic growth under different RH conditions*

The effect of water vapor on aerosol scattering was examined, in order to explain the difference in the variations of $PM_{2.5}$ mass concentrations and visibility. A new empirical relationship between RH and f_{550nm}(RH), the ratio of ambient extinction coefficient to aerosol dry scattering coefficient, was built to characterize the aerosol hygroscopicity. Considering the large variation in RH and the duration of high RH during the experiment, the observational period was classified into different periods according to the ambient RH condition.

A distinct diurnal cycle of RH can be seen in Fig. 2. To analyze the high RH condition and its impact on aerosol hygroscopic growth, a new parameter, $d_{80\%,24h}$, was defined to quantitatively characterize the occurrence of high humidity conditions (> 80%) during the last 24 h:

$$d_{\mathrm{RH}_0,\Delta t}(t) = \overline{\mathrm{RH}(\mathrm{RH} > \mathrm{RH}_0, t-\Delta t < T \leqslant t)} - \mathrm{RH}_0 \frac{1}{1-\mathrm{RH}_0}, \tag{5}$$

where $\mathrm{RH}(\mathrm{RH} > \mathrm{RH}_0, t-\Delta t < T \leqslant t)$ is the RH above a threshold RH (RH_0) during the previous Δt period, overbar represents average throughout the given period, and the fraction on the right ensures that the result is within the RH

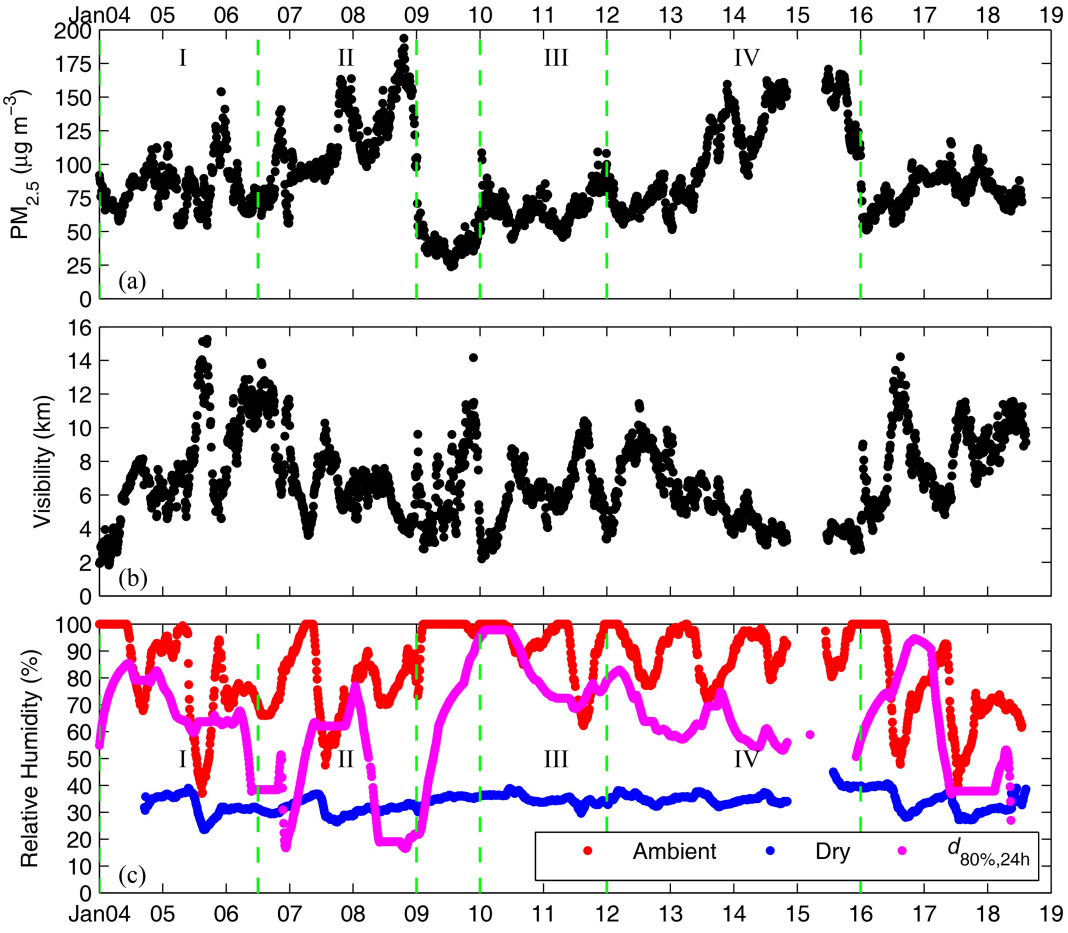

Fig. 2. Observation of $PM_{2.5}$, visibility, RH and $d_{80\%,24h}$.

range, i.e., 0%–100%. A high $d_{RH_0,\Delta t}$ might suggest a favorable situation for heterogeneous reactions at high RH for a long time. As a result, trace gases such as SO_2 and NO_x from industries near the experimental site and other emission sources could be more easily heterogeneously oxidized to form sulfates and nitrates. In other words, a high $d_{RH_0,\Delta t}$ means a long duration of high moisture leading to a stronger hygroscopic growth ability of aerosol.

Each of the two pollution episodes could be further divided into two periods (Fig. 2c). It was noted that $d_{RH_0,\Delta t}$ decreased similarly from the first period to the second period during each episode, showing that aerosols firstly went through a humid condition and then a relatively dry condition. Figure 4 shows the simplified hygroscopic enhancement factor, f_{550nm}(RH), which was typically below 1.2, representing very weak hygroscopic growth when RH was below 60%. The f_{550nm}(RH) increased steeply with RH above 80%. The scattering of particles could be enhanced by 1.5–3 times when ambient RH was above 90%. The dual-parameter fit [Eq. (4)] was applied and the fit parameters of γ were 0.201, 0.180, 0.222 and 0.174 for the four periods, respectively. Clearly, γ was higher for the periods with high $d_{80\%,24h}$ (Ⅰ and Ⅲ), indicating efficient aging due to multi-phase reactions and the production of soluble inorganic salts. The $d_{80\%,24h}$ was lower for the other two periods (Ⅱ and Ⅳ), indicating less efficient aging by soluble inorganic salts. However, the aerosol mass concentration could still accumulate via condensation of organic species, which was the main emission of the surrounding industrial park and might have resulted in smaller aerosol hygroscopicity.

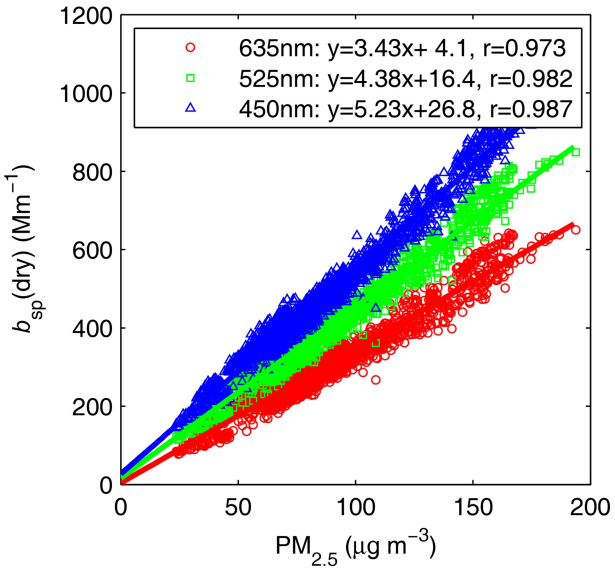

Fig. 3. Linear relationship between $PM_{2.5}$ mass concentration and scattering coefficient at three wavelengths.

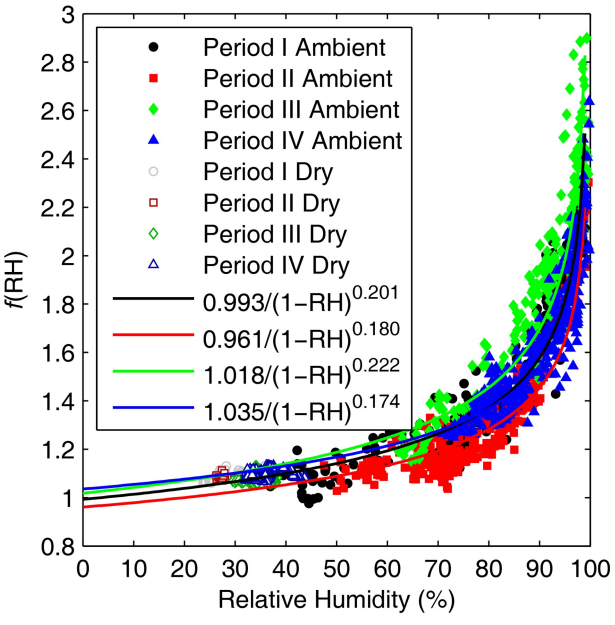

Fig. 4. f(RH) in four periods and the fitted function.

Pan et al. (2009) reported f_{525nm} (80%) values of 1.20, 1.31 and 1.57 during dust, clean and pollution episodes over a rural area near the megacity of Beijing. Zhao et al. (2019) performed a survey of f_λ(RH) studies in China for the past seven years. In winter, the f_{550nm} (80%) of Gucheng, f_{525nm} (80%) of Beijing and f_{525nm} (80%) of Guangzhou was 1.29 ± 0.10, 1.47 ± 0.16, and 1.58 ± 0.07, respectively. In this study, the f_{550nm} (80%) for the above mentioned four segments ranged from 1.28–1.46, which was a similar range to other studies.

3.3. *Relationship between $PM_{2.5}$ mass concentration and visibility*

The relationship between $PM_{2.5}$ mass concentration and visibility is subject to the RH conditions owing to the hygroscopic growth of aerosols. The establishment of an empirical relationship between $PM_{2.5}$ mass concentration and visibility under different RH conditions would be useful for estimating $PM_{2.5}$ mass concentrations based on visibility—a widely measured parameter.

In the IMPROVE algorithm, the computed aerosol light extinction coefficients include contributions from $PM_{2.5}$ species such as ammonium sulfate, ammonium nitrate, organic matter, elemental carbon, fine soil, coarse mass, and Rayleigh scattering, as well as the hygroscopic enhancement factor f_λ(RH) (Ryan et al., 2005). The equation requires knowledge of mass concentrations of different components, which are not always available or only measured at low temporal resolution. Since the light extinction at the observational site is mainly contributed by $PM_{2.5}$, we can simply calculate the extinction coefficient at ambient RH using the following equation:

$$\begin{aligned} b_{ext,\lambda}(\mathrm{RH}) &= f_\lambda(\mathrm{RH}) b_{sp,\lambda}(\mathrm{dry}) \\ &= f_\lambda(\mathrm{RH})(\alpha_{PM_{2.5},\lambda}[PM_{2.5}]+\varepsilon), \end{aligned} \tag{6}$$

where the contribution of $PM_{2.5}$ mass concentration is considered using a mass scattering efficiency, $\alpha_{PM_{2.5},\lambda}$, and others are written as ε. The linear relationship between $PM_{2.5}$ mass concentration and the dry scattering coefficient, b_{sp}, is built based on the observation. Figure 3 shows the linearly fit-

ted results at three wavelengths (450, 525 and 635 nm). The mass scattering efficiency at the site is 4.127 $m^2\ g^{-1}$ (550 nm), which is close to but a little higher than that in the IMPROVE equation.

From the combination of Eqs. (2) and (5), the relationship between $PM_{2.5}$ mass concentration and measured visibility under a given RH can be obtained as Eq. (7):

$$PM_{2.5}=\frac{1}{f_\lambda(\mathrm{RH})\alpha_{PM_{2.5},\lambda}}\left(\frac{3.91}{V}\left(\frac{\lambda}{0.55}\right)^{-q}-\varepsilon f_\lambda(\mathrm{RH})\right). \quad (7)$$

Figure 5 compares the measured and regressed $PM_{2.5}$ mass concentrations in two ways—one using f_λ(RH) in four periods, and the other using the average f_λ(RH) during the whole observational period, $1.030 / (1 - \mathrm{RH})^{0.183}$. The results show that simulated $PM_{2.5}$ mass concentrations from both methods coincide well with the measurements. The slopes of the two methods are 0.93 and 0.94 respectively, and the intercepts are 6.6 and 8. The correlation coefficient of the first method is 0.89, which is better than the second one at 0.81.

4. Conclusions

Particulate matter, such as $PM_{2.5}$, has recently drawn the attention of the public. Although more and more monitoring sites have been built, the total number is still limited and the sites are relatively dense only in urban areas. In addition to direct measurements of particulate matter, visibility measurements are available at many stations, covering different terrain and regions. Satellites provide aerosol optical properties for a vast space, and these optical measurements could fill in the missing parts in the monitoring of particulate matter. Thus, it is worth investigating the relationship between $PM_{2.5}$ mass concentration and optical properties in order to derive a simplified method to estimate and establish a nationwide map of $PM_{2.5}$ mass concentration. In this study, a field campaign was conducted in Southwest China in January 2019 to explore the relationship of $PM_{2.5}$ mass concentrations, visibility (ambient aerosol extinction) and RH.

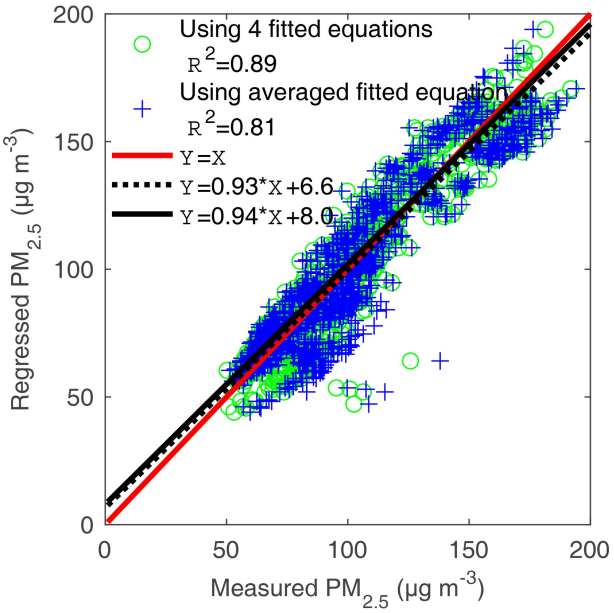

Fig. 5. Comparison between measured $PM_{2.5}$ mass concentration and regressed $PM_{2.5}$ mass concentration via two methods (black solid line—using four fitted equations; black dotted line—using averaged fitted equation).

Two pollution episodes were encountered during the campaign. For each episode, a good linear relationship of $PM_{2.5}$ mass concentration and dry aerosol scattering coefficient was found. However, the linear correlation between $PM_{2.5}$ mass concentration and visibility is only about 0.21, which indicates that ambient RH has an important effect on visibility. Each episode was further divided into two periods—the first one with high aerosol hygroscopicity and high RH, and the second one with a relatively dry but more polluted condition and low aerosol hygroscopicity.

Based on the established empirical relationship between the hygroscopic enhancement factor, f_λ(RH), the ratio of ambient aerosol extinction coefficient to dry aerosol scattering coefficient, and RH, a simplified method for predicting the $PM_{2.5}$ mass concentrations from measurements of visibility and RH was developed and verified. This method is applicable for other regions to generate their own empirical relationships using related data. Although nephelometers are not so densely equipped as instruments for visibility or $PM_{2.5}$ mass concentration measurements, available observations at representative stations could be used to generate parameters in different regions and under different conditions for the proposed parameterization scheme. $PM_{2.5}$ mass concentration could also be estimated using the AOD from satellite or sunphotometer measurements, except that the vertical distribution of aerosol properties and RH has to be taken into consideration. Profiles of $PM_{2.5}$ mass concentration could also be obtained based on a similar method. Therefore, this method would be useful for the remote sensing of $PM_{2.5}$ mass concentrations.

Acknowledgements. This research was supported by a National Science and Technology Major Project (Grant No. 2016YFC 0200403) and the National Natural Science Foundation of China (Grant Nos. 41675037 and 41675038).

REFERENCES

Carrico, C. M., P. Kus, M. J. Rood, P. K. Quinn, and T. S. Bates, 2003: Mixtures of pollution, dust, sea salt, and volcanic aerosol during ACE-Asia: Radiative properties as a function of relative humidity. *J. Geophys. Res.*, **108**, 8650, https://doi.org/

10.1029/2003JD003405.

Chan, C. K., and X. H. Yao, 2008: Air pollution in mega cities in China. *Atmos. Environ.*, **42**, 1–42, https://doi.org/10.1016/j.atmosenv.2007.09.003.

Chan, Y. C., R. W. Simpson, G. H. Mctainsh, P. D. Vowles, D. D. Cohen, and G. M. Bailey, 1999: Source apportionment of visibility degradation problems in Brisbane (Australia) using the multiple linear regression techniques. *Atmos. Environ.*, **33**, 3237–3250, https://doi.org/10.1016/S1352-2310(99)00091-6.

Chelani, A. B., 2019: Estimating $PM_{2.5}$ concentration from satellite derived aerosol optical depth and meteorological variables using a combination model. *Atmospheric Pollution Research*, **10**, 847–857, https://doi.org/10.1016/j.apr.2018.12.013.

Chen, J., and Coauthors, 2019: Aerosol hygroscopic growth, contributing factors, and impact on haze events in a severely polluted region in northern China. *Atmospheric Chemistry and Physics*, **19**, 1327–1342, https://doi.org/10.5194/acp-19-1327-2019.

Collaud Coen, M., and Coauthors, 2010: Minimizing light absorption measurement artifacts of the Aethalometer: Evaluation of five correction algorithms. *Atmospheric Measurement Techniques*, **3**, 457–474, https://doi.org/10.5194/amt-3-457-2010.

Ding, M. Z., A. L. Chen, and Y. S. Ni, 2014: Several observation methods of PM_{10}, $PM_{2.5}$. *Journal of Zhejiang Meteorology*, **35**(4), 44–46, https://doi.org/10.16000/j.cnki.zjqx.2014.04.010. (in Chinese)

Gassó, S., and Coauthors, 2000: Influence of humidity on the aerosol scattering coefficient and its effect on the upwelling radiance during ACE-2. *Tellus B*, **52**, 546–567, https://doi.org/10.3402/tellusb.v52i2.16657.

Hänel, G., 1976: The properties of atmospheric aerosol particles as functions of the relative humidity at thermodynamic equilibrium with the surrounding moist air. *Advances in Geophysics*, **19**, 73–188, https://doi.org/10.1016/S0065-2687(08)60142-9.

Hänel, G., 1980: An attempt to interpret the humidity dependencies of the aerosol extinction and scattering coefficients. *Atmos. Environ.*, **15**, 403–406, https://doi.org/10.1016/0004-6981(81)90045-7.

Hansen, A. D. A., H. Rosen, and T. Novakov, 1984: The aethalometer–An instrument for the real-time measurement of optical absorption by aerosol particles. *Science of the Total Environment*, **36**, 191–196, https://doi.org/10.1016/0048-9697(84)90265-1.

Kan, H. D., R. J. Chen, and S. L. Tong, 2012: Ambient air pollution, climate change, and population health in China. *Environment International*, **42**, 10–19, https://doi.org/10.1016/j.envint.2011.03.003.

Kasten, F., 1969: Visibility forecast in the phase of pre-condensation. *Tellus*, **21**, 631–635, https://doi.org/10.3402/tellusa.v21i5.10112.

Kotchenruther, R. A., and P. V. Hobbs, 1998: Humidification factors of aerosols from biomass burning in Brazil. *J. Geophys. Res.*, **103**, 32 081–32 089, https://doi.org/10.1029/98jd00340.

Li, C. C., X. He, Z. Z. Deng, A. K. H. Lau, and Y. Li, 2013: Dependence of mixed aerosol light scattering extinction on relative humidity in Beijing and Hong Kong. *Atmos. Ocean. Sci. Lett.*, **6**, 117–121, https://doi.org/10.1080/16742834.2013.11447066.

Liu, F., Q. W. Tan, X. Jiang, F. M. Yang, and W. J. Jiang, 2019: Effects of relative humidity and $PM_{2.5}$ chemical compositions on visibility impairment in Chengdu, China. *Journal of Environmental Sciences*, **86**, 15–23, https://doi.org/10.1016/j.jes.2019.05.004.

Malm, W. C., and D. E. Day, 2001: Estimates of aerosol species scattering characteristics as a function of relative humidity. *Atmos. Environ.*, **35**, 2845–2860, https://doi.org/10.1016/s1352-2310(01)00077-2.

Müller, T., and Coauthors, 2011: Characterization and intercomparison of aerosol absorption photometers: Result of two intercomparison workshops. *Atmospheric Measurement Techniques*, **4**, 245–268, https://doi.org/10.5194/amt-4-245-2011.

Pan, X. L., P. Yan, J. Tang, J. Z. Ma, Z. F. Wang, A. Gbaguidi, and Y. L. Sun, 2009: Observational study of influence of aerosol hygroscopic growth on scattering coefficient over rural area near Beijing mega-city. *Atmospheric Chemistry and Physics*, **9**, 7519–7530, https://doi.org/10.5194/acp-9-7519-2009.

Pandolfi, M., and Coauthors, 2018: A European aerosol phenomenology-6: Scattering properties of atmospheric aerosol particles from 28 ACTRIS sites. *Atmospheric Chemistry and Physics*, **18**, 7877–7911, https://doi.org/10.5194/acp-18-7877-2018.

Pui, D. Y. H., S. C. Chen, and Z. L. Zuo, 2014: $PM_{2.5}$ in China: Measurements, sources, visibility and health effects, and mitigation. *Particuology*, **13**, 1–26, https://doi.org/10.1016/j.partic.2013.11.001.

Ran, L., Z. Z. Deng, P. C. Wang, and X. A. Xia, 2016: Black carbon and wavelength-dependent aerosol absorption in the North China Plain based on two-year aethalometer measurements. *Atmos. Environ.*, **142**, 132–144, https://doi.org/10.1016/j.atmosenv.2016.07.014.

Ryan, P. A., D. Lowenthal, and N. Kumar, 2005: Improved light extinction reconstruction in interagency monitoring of protected visual environments. *Journal of the Air & Waste Management Association*, **55**, 1751–1759, https://doi.org/10.1080/10473289.2005.10464768.

Song, M., S. Q. Han, M. Zhang, Q. Yao, and B. Zhu, 2013: Relationship between visibility and relative humidity, PM_{10}, $PM_{2.5}$ in Tianjin. *Journal of Meteorology and Environment*, **29**, 34–41, https://doi.org/10.3969/j.issn.1673-503X.2013.02.006. (in Chinese)

Sun, J. Y., L. Zhang, X. J. Shen, H. C. Che, Y. M. Zhang, R. X. Fan, Q. L. Ma, Y. Yue, and X. M. Yu, 2016: A review of the effects of relative humidity on aerosol scattering properties. *Acta Meteorologica Sinica*, **74**(5), 672–682. (in Chinese)

Sun, Y. B., Q. L. Zeng, B. Geng, X. W. Lin, B. Sude, and L. F. Chen, 2019: Deep learning architecture for estimating hourly ground-level $PM_{2.5}$ using satellite remote sensing. *IEEE Geoscience and Remote Sensing Letters*, **16**, 1343–1347, https://doi.org/10.1109/LGRS.2019.2900270.

van Donkelaar, A., R. V. Martin, and R. J. Park, 2006: Estimating ground - level $PM_{2.5}$ using aerosol optical depth determined from satellite remote sensing. *J. Geophys. Res.*, **111**, D21201, https://doi.org/10.1029/2005JD006996.

Wang, Y. H., Z. R. Liu, J. K. Zhang, B. Hu, D. S. Ji, Y. C. Yu, and Y. S. Wang, 2015: Aerosol physicochemical properties and implications for visibility during an intense haze episode during winter in Beijing. *Atmospheric Chemistry and Physics*, **15**, 3205–3215, https://doi.org/10.5194/acp-15-3205-2015.

Watson, J. G., 2002: Visibility: Science and regulation. *Journal*

of the Air & Waste Management Association, **52**, 628–713, https://doi.org/10.1080/10473289.2002.10470813.

Xu, L., 2017: The comparison research on determination of $PM_{2.5}$ and PM_{10} concentration by light scattering method and β-ray method. *Environment and Development*, **29**(6), 97–99, https://doi.org/10.16647/j.cnki.cn15-1369/X.2017.06.062. (in Chinese)

Zhang, R. H., Q. Li, and R. N. Zhang, 2014: Meteorological conditions for the persistent severe fog and haze event over eastern China in January 2013. *Science China Earth Sciences*, **57**, 26–35, https://doi.org/10.1007/s11430-013-4774-3.

Zhao, C. S., Y. L. Yu, Y. Kuang, J. C. Tao, and G. Zhao, 2019: Recent progress of aerosol light-scattering enhancement factor studies in China. *Adv. Atmos. Sci.*, **36**, 1015–1026, https://doi.org/10.1007/s00376-019-8248-1.

Zheng, C., and Coauthors, 2017: Analysis of influential factors for the relationship between $PM_{2.5}$ and AOD in Beijing. *Atmospheric Chemistry and Physics*, **17**, 13 473–13 489, https://doi.org/10.5194/acp-17-13473-2017.

Zhou, M., and Coauthors, 2016: Chemical characteristics of fine particles and their impact on visibility impairment in Shanghai based on a 1-year period observation. *Journal of Environmental Sciences*, **48**, 151–160, https://doi.org/10.1016/j.jes.2016.01.022.

Zieger, P., and Coauthors, 2011: Comparison of ambient aerosol extinction coefficients obtained from in-situ, MAX-DOAS and LIDAR measurements at Cabauw. *Atmospheric Chemistry and Physics*, **11**, 2603–2624, https://doi.org/10.5194/acp-11-2603-2011.